FULL PAPER

Dalton
www.rsc.org/dalton

Organic–inorganic hybrids of imidazole complexes of palladium(II), copper(II) and zinc(II). Crystals and liquid crystals†

Ching Kuan Lee, Mei Jing Ling and Ivan J. B. Lin*

Department of Chemistry, National Dong Hwa University, Shoufeng, Hualien 974, Taiwan. E-mail: ijblin@mail.ndhu.edu.tw

Received 24th July 2003, Accepted 24th September 2003
First published as an Advance Article on the web 20th October 2003

Neutral and ionic complexes of organic–inorganic hybrids having general formulas of $[M(C_nH_{2n+1}\text{-im})_2Cl_2]$ (C_nH_{2n+1}-im, represents *N*-alkyl substituted imidazoles; n = 10, 12 and 18 for M = Pd(II); n = 12 and 18 for M = Cu(II) and Zn(II)) and $[M(C_nH_{2n+1}\text{-im})_4][NO_3]_2$ (for M = Cu(II), Zn(II), n = 10, 12, 14, 16 and 18), have been investigated. Three neutral compounds, $[Pd(C_{12}H_{25}\text{-im})_2Cl_2]$, $[Cu(C_{12}H_{25}\text{-im})_2Cl_2]$ and $[Zn(C_{18}H_{37}\text{-im})_2Cl_2]$ and one ionic compound $[Cu(C_{12}H_{25}\text{-im})_4][NO_3]_2$ were structurally determined by single crystal X-ray diffraction. Among them, the Zn(II) compound is tetrahedral and the others are square planar. Among the neutral compounds synthesized, only the zinc compound with n = 18 exhibits liquid crystalline behavior upon cooling from isotropic liquid. All the ionic Zn(II) compounds exhibit SmA mesophases, except that with n = 10, which is a room-temperature ionic liquid. Ionic Cu(II) compounds exhibit a highly ordered lamellar mesophase.

Introduction

Organic–inorganic hybrid materials have received considerable interest because of the potential of having mixed organic and inorganic features.[1–4] Through suitable combinations, materials with new properties can be obtained. For example, thin films composed of metal or metal ions are important materials having characteristic properties such as electrical conductivity, magnetism and carrier mobility, to name a few.[1,5–7] Organic–inorganic hybrids formed through incorporation of soft organic portions into metal ions can not only tune the electrical, optical and structural properties, but also allow the hybrids to be processed conveniently. As another example, either naturally occurring or man-made, liquid crystalline materials are both scientifically and industrially important; introducing metal ions to liquid crystalline materials generates an important class of organic–inorganic hybrid, metallomesogens.[8] Metallomesogens which are metal containing liquid crystals possess many interesting properties. The presence of metal ions can induce the transition of some non-mesogenic compounds to mesogenic compounds. Metal ions are also known to have a variety of geometries; therefore metallomesogens may have new geometrical shapes, which may not be obtained in conventional organic liquid crystals. Moreover, the richness in oxidation state, color, and magnetism possessed by metal ions are additional properties of metallomesogens. Metallomesogens not only have the advantages of being organic–inorganic hybrids but also have the advantage of being easy to process through self-assembly to form layered thin films.

Being a stronger base than pyridine, imidazole is a versatile ligand for the formation of metal complexes. However, examples of imidazole–metal complexes of organic–inorganic hybrids are rare. To the best of our knowledge, no imidazole containing metallomesogens have been reported. Closely related imidazolium and pyridinium tetrahalometallates(II), which exhibit a rich liquid crystalline behaviour, are known.[9] In this paper we report the crystal and liquid crystal properties of imidazole complexes of Pd(II), Cu(II) and Zn(II). Liquid crystalline compounds reported in this work exhibit lamellar structures in the mesophase.

† Electronic supplementary information (ESI) available: Supplementary NMR and EA data. Table 1: Crystal data for $[Cu(C_{12}H_{25}\text{-im})_4][NO_3]_2$. Fig. S1: ORTEP drawing of $[Cu(C_{12}H_{25}\text{-im})_4]^{2+}$ with partial atomic numberings, hydrogens being omitted for clarity. Fig. S2: The crystal packing of $[Cu(C_{12}H_{25}\text{-im})_4][NO_3]_2$ viewing along the *b*-axis. See http://www.rsc.org/suppdata/dt/b3/b308648h/

Result and discussion

Synthesis and characterization of complexes

The ligands were synthesized according to the literature methods.[10] Neutral compounds having a general formula of $[M(C_nH_{2n+1}\text{-im})_2Cl_2]$, ($C_nH_{2n+1}$-im represents 1-alkylimidazole with alkyl = C_nH_{2n+1}, n = 10, 12, 18 for M = Pd(II); n = 12, 18 for M = Cu(II) and Zn(II)) were prepared by the reaction of two equivalents of 1-alkylimidazole with one equivalent of metal halide (see Scheme 1). Identical products were obtained even when excess ligand (up to four molar ratios) was employed. Ionic compounds of Cu(II) and Zn(II) having the general formula of $[M(C_nH_{2n+1}\text{-im})_4][NO_3]_2$ (n = 10, 12, 14, 16 and 18 for M = Zn(II) and Cu(II), the ionic Zn(II) compounds contain one or two crystallization water molecules) were prepared by the reaction of four equivalents of ligand with one equivalent of metal nitrate (see Scheme 1). All the complexes are reasonably soluble in THF, CH_2Cl_2, ethanol and acetone. The solubility, however, decreases with increasing alkyl chain length. Other things being equal, the neutral Pd(II) complexes are the least soluble, while those of the ionic Zn(II) compounds are the most soluble. The ionic Zn(II) compounds, especially the lower homologues, even dissolve in hexane and ether. ^{1}H NMR spectroscopy and elemental analyses were used to characterize and confirm the identity of the metal complexes. Upon complexation, downfield shifts of the ^{1}H chemical shifts of the imidazole ring protons and the NCH_2 protons by several ppm with respect to those of the free ligands are observed. The ionic Zn(II) compounds are very hygroscopic. Freshly prepared products always contain hydrated water. These hydrates can be dehydrated under vacuum at 80 °C for 12 h. Exposure to air or even storage in sample vials causes the dried samples to become hydrates and this can be easily followed by thermal gravimetric analysis. Elemental analyses indicate that all the compounds have the correct C/N ratios. While most of the ionic Zn(II) compounds are monohydrates, the one with n = 18 is a dihydrate.

Plate-like orange crystals of $[Pd(C_{12}H_{25}\text{-im})_2Cl_2]$ suitable for single crystal X-ray diffraction were obtained by recrystallization from dichloromethane–acetone. This compound crystallized in the monoclinic space group having two molecules in the unit cell (see Table 1 for crystallographic data). The palladium atom is in a special position. The square-planar geometry around the palladium is formed by two Cl^- and two N-coordinated imidazoles (Fig. 1(a)). The two *trans* imidazole ring planes are tilted by ~30° from the square plane. In each imidazole ligand the alkyl chain is tilted 42.3° from the imidazole

DOI: 10.1039/b308648h

Table 1 Summary of crystallographic data for $[Pd(C_{12}H_{25}\text{-im})_2Cl_2]$, $[Cu(C_{12}H_{25}\text{-im})_2Cl_2]$ and $[Zn(C_{18}H_{37}\text{-im})_2Cl_2]$

	$[(C_{12}H_{25}\text{-im})_2PdCl_2]$	$[(C_{12}H_{25}\text{-im})_2CuCl_2]$	$[(C_{18}H_{37}\text{-im})_2ZnCl_2]$
Empirical formula	$C_{30}H_{56}Cl_2N_4Pd$	$C_{30}H_{56}Cl_2CuN_4$	$C_{42}H_{80}Cl_2N_4Zn$
M_r	650.13	607.23	777.37
T/K	296(2)	293(2)	293(2)
λ/Å	0.71073	0.71073	0.71073
Crystal system	Monoclinic	Triclinic	Triclinic
Space group	$P2_1/n$	$P\bar{1}$	$P\bar{1}$
Unit cell dimensions:			
a/Å	4.7995(5)	8.3007(10)	8.221(3)
b/Å	44.832(5)	10.732(2)	11.8579(12)
c/Å	7.7472(8)	19.3765(18)	24.346(3)
α/°	90	77.929(10)	82.486(7)
β/°	94.345(2)	89.330(8)	81.457(12)°
γ/Å	90	87.332(16)	84.442(12)
V/Å^3	1662.2(3)	1686.2(5)	2319.5(8)
Z	2	2	2
D_c/Mg m^{-3}	1.299	1.196	1.113
μ/mm^{-1}	0.743	0.830	0.675
F(000)	688	654	848
Crystal size/mm	0.30 × 0.20 × 0.10	0.9 × 0.7 × 0.2	0.4 × 0.2 × 0.1
θ Range for data collection/°	0.91–28.29	1.07–25.00	1.84–22.50
Index ranges, hkl	−6 to 5, −49 to 59, −9 to 10	−9 to 0, −12 to 12, −23 to 23	−8 to 0, −12 to 12, −26 to 25
Reflections collected	10552	6062	6543
Independent reflections (R_{int})	3981 (0.0496)	5627 (0.0162)	6034 (0.0452)
Data/restraints/parameters	3981/0/169	5627/0/334	6034/0/442
Goodness-of-fit on F^2	0.994	1.082	0.916
Final R indices [$I > 2\sigma(I)$]	$R1 = 0.0480$, $wR2 = 0.0881$	$R1 = 0.0382$, $wR2 = 0.0983$	$R1 = 0.0749$, $wR2 = 0.1840$
R Indices (all data)	$R1 = 0.1077$, $wR2 = 0.1159$	$R1 = 0.0499$, $wR2 = 0.1052$	$R1 = 0.1709$, $wR2 = 0.2562$

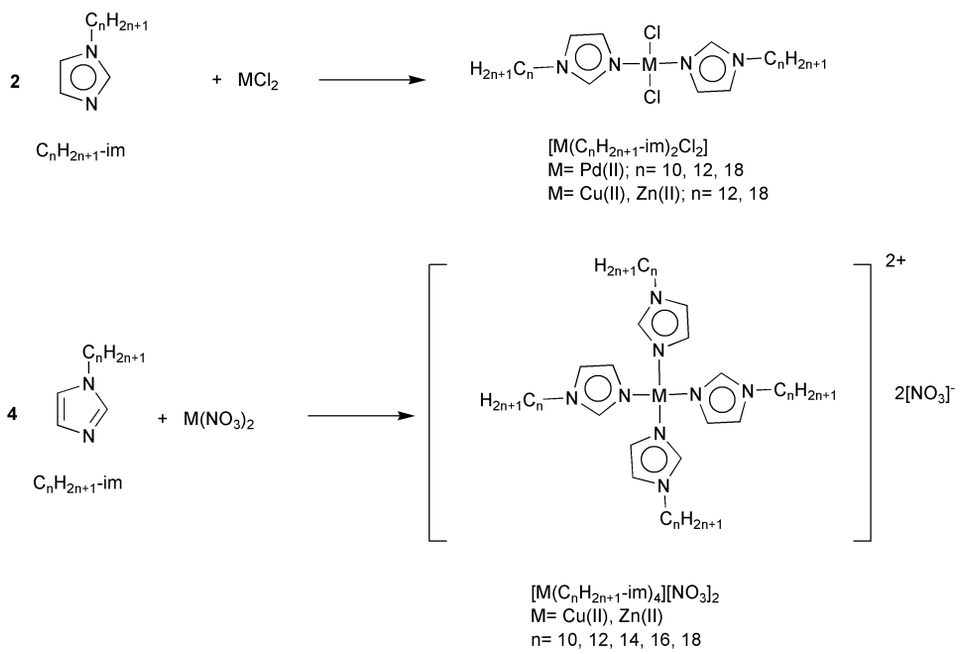

Scheme 1

ring plane. The two alkyl chains in the molecule point in opposite directions. The molecules are packed in a highly interdigitated monolayer fashion with a repeating layer distance of ~22 Å (Fig. 1(b)).

Deep blue crystals of $[Cu(C_{12}H_{25}\text{-im})_2Cl_2]$ suitable for single crystal X-ray diffraction were grown from acetone. The structure of this neutral Cu(II) compound is similar to that of $[Pd(C_{12}H_{25}\text{-im})_2Cl_2]$. The square-planar geometry around the copper is formed by two Cl^- and two N-coordinated imidazoles (Fig. 2(a)). The twist angle between the two *trans* imidazole rings is 20°. One of the imidazole planes is tilted by 13° from the square plane, the other is tilted by 33°. The long alkyl chains do not lie parallel to the imidazole ring but are tilted 37° and 32° from the ring plane. Similar to the Pd(II) compound, the two alkyl chains in the molecule point in opposite directions. The crystal packing diagram of this neutral Cu(II) compound is also similar to that of the Pd(II) compound, a highly interdigitated monolayer stacking being adopted (Fig. 2(b)). The repeating distance of this monolayer structure is ~19 Å, which is shorter than for the corresponding Pd(II) compound.

The molecular structure of $[Zn(C_{18}H_{37}\text{-im})_2Cl_2]$ is shown in Fig. 3(a). The Zn(II) center adopts a tetrahedral geometry. The bond angles around the zinc(II) ion are N(4)–Zn(1)–N(2) 110.1(3)°, N(4)–Zn(1)–Cl(2) 106.7(2)°, N(2)–Zn(1)–Cl(2) 107.8(2)°, N(4)–Zn(1)–Cl(1) 106.8(2)°, N(2)–Zn(1)–Cl(1) 106.6(2)°, Cl(2)–Zn(1)–Cl(1) 119.02(11)°. In one of the two imidazole ligands, the alkyl chain is tilted by 19° from the imidazole ring plane, and in the other ligand, the alkyl chain is perpendicular (91°) to the imidazole ring plane. Molecules of this compound are packed in an interdigitated bilayer fashion (Fig. 3(b)). The repeating distance of this monolayer packing is ~24 Å.

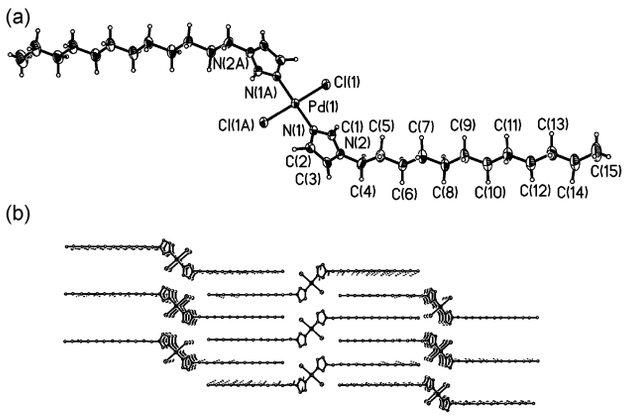

Fig. 1 (a) ORTEP drawing[11] of $[Pd(C_{12}H_{25}\text{-im})_2Cl_2]$ (30% thermal ellipsoids) with partial atomic numbering. (b) The crystal packing of $[Pd(C_{12}H_{25}\text{-im})_2Cl_2]$ viewed along the *a*-axis.

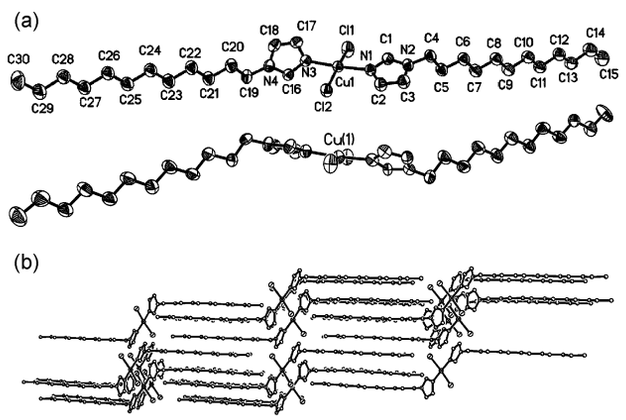

Fig. 2 (a) ORTEP drawing[11] of $[Cu(C_{12}H_{25}\text{-im})_2Cl_2]$ (30% thermal ellipsoids) with partial atomic numbering, hydrogens being omitted for clarity. (b) The crystal packing of $[Cu((C_{12}H_{25})_2\text{-im})_2Cl_2]$.

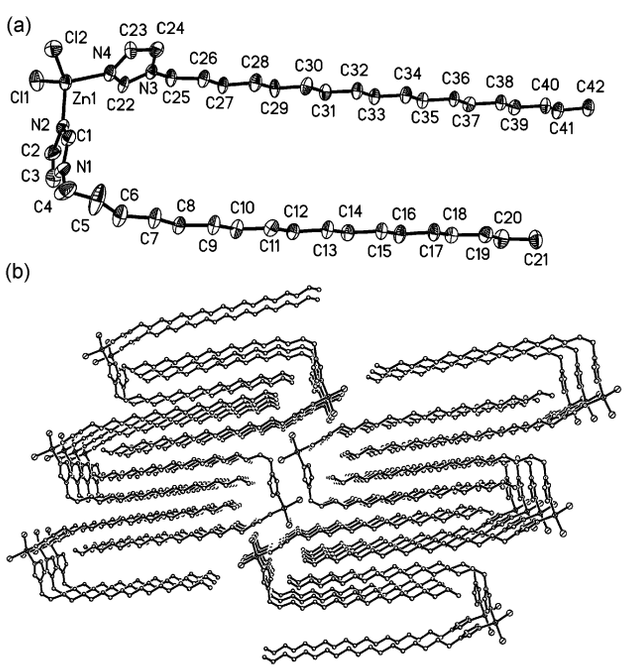

Fig. 3 (a) ORTEP drawing[11] of $[Zn(C_{18}H_{37}\text{-im})_2Cl_2]$ (30% thermal ellipsoids) with partial atomic numbering, hydrogens being omitted for clarity. (b) The bilayer crystal packing of $[Zn(C_{18}H_{37}\text{-im})_2Cl_2]$ viewing along the *a*-axis.

Thin purple crystals of $[Cu(C_{12}H_{25}\text{-im})_4][NO_3]_2$ were recrystalized from dichloromethane–acetone. The quality of crystals is poor, such that the thermal motion of two alkyl chains is very large. Despite the poor result of the structure resolved, the major scheme of this structure is basically correct. The Cu(II) atom again adopts a square-planar geometry. A crystal packing diagram shows that the four alkyl chains are packed biradially. Two of the four alkyl chains are twisted around to fit into this biradial packing diagram. The molecular cation of this compound stacks in a non-interdigitated monolayer fashion (see ESI †). The repeating distance of the monolayer is ~26 Å.

The thermal behaviors of these complexes were studied by differential scanning calorimetry (DSC), polarized optical microscopy (POM) and powder X-ray diffraction (XRD). The phase transition temperatures and thermodynamic data for the neutral compounds are summarized in Table 2.

DSC thermograms of the neutral imidazole complexes of Pd(II) show that the transition temperatures of melting increase upon increasing the chain length. The melting temperature of $[Pd(C_{10}H_{21}\text{-im})_2Cl_2]$ is 105.9 °C. When the chain lengths increase to 12 and 18, the melting points are 111.9 and 119.7 °C, respectively. The enthalpies of melting increase upon increasing the chain length and have an average value of 3.4 kJ mol^{-1} per carbon. The compounds $[Cu(C_nH_{2n+1}\text{-im})_2Cl_2]$ (n = 12, 18) have a lower but similar trend of melting temperature (78.0 and 97.8 °C) and enthalpy value as compared to the Pd(II) series. When the metal ion is changed to Zn(II), the geometry of the metal center changes to tetrahedral. The melting points for the Zn(II) compounds are 95.6 (n = 12) and 108.9 °C (n = 18). Interestingly, upon cooling from the isotropic liquid, the complex $[Zn(C_{18}H_{37}\text{-im})_2Cl_2]$ displays liquid crystalline behavior. The cooling DSC thermogram of this compound shows a small exothermic process (1.6 kJ mol^{-1}) at 95.5 °C and a relatively large exothermic process (66.3 kJ mol^{-1}) at 73.5 °C. The small ΔH value indicates a transition from an isotropic phase to a disordered phase. POM observation of this compound reveals a *batonnet* texture and homeotropic behavior. Results from DSC and POM, therefore suggest the presence of an SmA mesophase. The absence of mesomorphism for the neutral Pd(II) and Cu(II) complexes may be due to a too small anisotropy, which renders a weak core–core interaction. The presence of the monotropic phase in the Zn(II) (n = 18) complex may be due to a larger anisotropy caused by its U-shape geometry.

The ionic Zn(II) compounds, except that with n = 10, all exhibit liquid crystal behavior (Table 3). Although the compound of n = 10 is non-mesogenic, it is, however, a room-temperature ionic liquid. The next higher homologous compound of n = 12 is a room-temperature liquid crystal and is thus also a partially ordered room-temperature ionic liquid. Phase transition data obtained from DSC were taken from the second heating cycle, which is different from the first heating cycle due to the process of dehydration. The clearing process of this compound (mesophase to isotropic liquid, M–I) occurs at 63.2 °C. For the compounds of n = 14, 16 and 18, the melting processes (crystal to mesophase, Cr–M) occur at 56.8, 58.0 and 62.5 °C, respectively. The corresponding phase transition temperatures of M–I are 79.0, 103.6 and 109.8 °C, respectively. The phase transition temperatures of Cr–M and M–I observed in this series of liquid crystalline compounds appear to increase upon increasing the carbon chain length. In this series of compounds, the dependence of the melting process on the chain length is greater than that of the clearing process. These liquid crystal compounds were also examined by POM. In the mesophase these compounds are viscous fluids, which exhibit typical fan-shape texture (Fig. 4(a)) and homeotropic behavior.

The mesomorphic structures of these compounds were further examined by XRD. The ionic Zn(II) compound of n = 12 is a room-temperature liquid crystalline material. The diffractogram of this compound exhibits two peaks at small angle region and a faint halo at medium angle (Fig. 4(b)). The small angle peaks measured at 28.2 and 14.0 Å are assigned to (001) and (002) reflections, respectively, and are an indication of layered structure with a repeating distance of 28.2 Å. The halo

Table 2 The phase transition (°C) temperatures of $[M(C_nH_{2n+1}\text{-im})_2Cl_2]$ (M = Pd(II), Cu(II), Zn(II)) complexes determined by DSC at a rate of 10 °C min^{-1} (enthalpy of transition in kJ mol^{-1} in parentheses) (Cr: crystal phase; SmA: smectic A; I: isotropic)

	n	Transition
$[Pd(C_nH_{2n+1}\text{-im})_2Cl_2]$	10	$Cr \underset{56.6(59.4)}{\overset{105.9(62.4)}{\rightleftharpoons}} I$
	12	$Cr \underset{77.4(77.3)}{\overset{111.9(81.2)}{\rightleftharpoons}} I$
	18	$Cr \underset{98.3(122.7)}{\overset{119.7(121.9)}{\rightleftharpoons}} I$
$[Cu(C_nH_{2n+1}\text{-im})_2Cl_2]$	12	$Cr \underset{<0}{\overset{78.0(71.5)}{\rightleftharpoons}} I$
	18	$Cr \underset{65.1(98.8)}{\overset{97.8(114.3)}{\rightleftharpoons}} I$
$[Zn(C_nH_{2n+1}\text{-im})_2Cl_2]$	12	$Cr \underset{55.5(51.2)}{\overset{95.6(51.3)}{\rightleftharpoons}} I$
	18	$Cr \underset{73.5(66.3)}{\overset{108.9(67.4)}{\rightleftharpoons}} SmA \underset{}{\overset{}{\rightleftharpoons}} I$ (95.5(1.6))

Table 3 The phase transition temperatures (°C) of $[M(C_nH_{2n+1}\text{-im})_4][NO_3]_2$ (M = Zn(II) and Cu(II)) complexes determined by DSC at rate of 10 °C min^{-1} (enthalpy of transition in kJ mol^{-1} in parentheses) (Cr: crystal phase; SmA: smectic A mesophase; SmX: highly ordered smectic phase: I: isotropic)

	n	Transition(s)
$[(C_nH_{2n+1}\text{-im})_4Zn][NO_3]_2$	10	Liquid
	12	$SmA \underset{59.6(2.9)}{\overset{63.2(2.9)}{\rightleftharpoons}} I$
	14	$Cr \underset{4.7(26.7)}{\overset{56.8(98.6)}{\rightleftharpoons}}$ $SmA \underset{76.5(5.0)}{\overset{79.0(5.0)}{\rightleftharpoons}} I$
	16	$Cr \underset{39.1(108.6)}{\overset{58.0(109.0)}{\rightleftharpoons}}$ $SmA \underset{99.7(5.8)}{\overset{103.6(5.7)}{\rightleftharpoons}} I$
	18	$Cr \underset{51.3(107.2)}{\overset{62.5(106.9)}{\rightleftharpoons}}$ $SmA \underset{106.5(5.8)}{\overset{109.8(5.8)}{\rightleftharpoons}} I$
$[(C_nH_{2n+1}\text{-im})_4Cu][NO_3]_2$	10	$Cr \underset{149.3(78.1)}{\overset{157.5(84.8)}{\rightleftharpoons}} I$
	12	$Cr \underset{68.3(20.6)}{\overset{74.6(20.6)}{\rightleftharpoons}}$ $SmX \underset{148.4(52.3)}{\overset{156.8(53.6)}{\rightleftharpoons}} I$
	14	$Cr \underset{67.6(6.2)}{\overset{72.9(10.4)}{\rightleftharpoons}}$ $SmX \underset{148.5(56.7)}{\overset{155.3(56.2)}{\rightleftharpoons}} I$
	16	$Cr \underset{67.4(32.1)}{\overset{71.4(33.3)}{\rightleftharpoons}}$ $SmX \underset{145.8(60.6)}{\overset{153.4(63.2)}{\rightleftharpoons}} I$
	18	$Cr \underset{68.0(54.9)}{\overset{72.8(57.1)}{\rightleftharpoons}}$ $SmX \underset{137.6(29.5)}{\overset{145.0(33.0)}{\rightleftharpoons}} I$

at ~4.5 Å indicates the fluid-like behavior of the alkyl chains. This diffraction pattern together with the fan-shape texture and homeotropic behavior from POM suggest the SmA mesophase. Diffractograms of the ionic Zn(II) compounds of $n = 14$, 16 and 18 in the mesophase have a similar pattern to that of $n = 12$. From XRD data, the deduced layer distances for each compound is 30.9, 32.5 and 35.5 Å, respectively. The layer spacings of these compounds are summarized in Table 4. A plot of these layer distances *vs.* carbon chain length *n* gives a straight line, suggesting similar structures in the mesophase. These observed layer distances are close to the expected molecular lengths with a tetrahedral geometry of biradial conformation. Therefore, a mesomorphic structure with non-interdigitated tetrahedral monolayer packing is proposed. This packing is similar to that of tetra-*n*-alkylammonium and phosphonium salts.[12]

Ionic compounds $[Cu(C_nH_{2n+1}\text{-im})_4][NO_3]_2$, with $n = 10$ is non-mesogenic, while those with $n = 12$, 14, 16 and 18 are mesogenic compounds. Upon melting, the crystalline solid of $n = 10$

Table 4 The *d*-spacings of $[M(C_nH_{2n+1}\text{-im})_4][NO_3]_2$ complexes from powder X-ray diffraction

		d-Spacing/Å (*T*/°C)	
M	*n*	Solid state	Mesophase
Zn	12	–	28.2 (30)
	14	23.5 (30)	30.9 (60)
	16	28.2 (30)	32.5 (85)
	18	30.7 (30)	35.5 (80)
Cu	12	26.4 (30)	28.0 (100)
	14	29.5 (30)	31.7 (100)
	16	–	35.5 (100)
	18	35.5 (30)	38.4 (100)

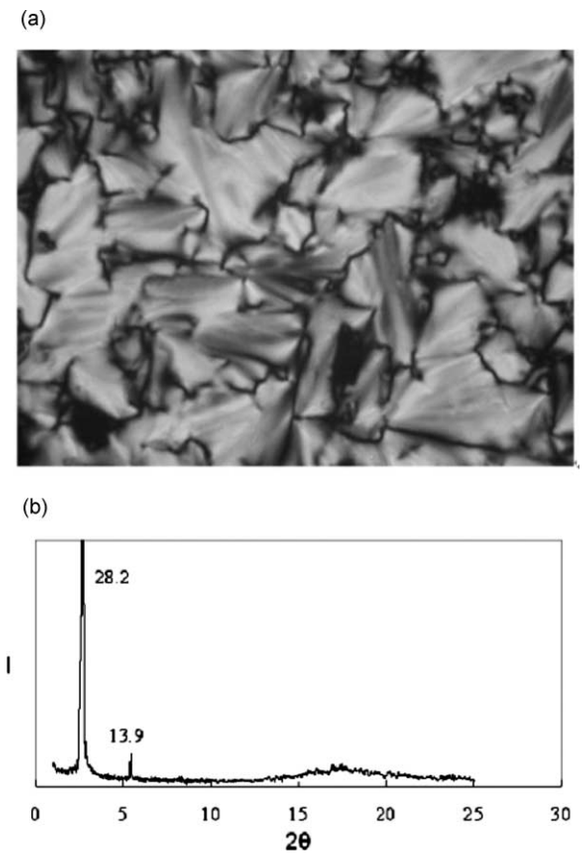

Fig. 4 (a) The fan texture of $[Zn(C_{12}H_{25}\text{-im})_4][NO_3]_2 \cdot H_2O$ at room temperature from POM. (b) Powder XRD of $[Zn(C_{12}H_{25}\text{-im})_4][NO_3]_2 \cdot H_2O$ at room temperature.

turns to an isotropic liquid, but those with $n = 12$, 14, 16 and 18 turn to jelly type materials, which under POM display mosaic texture with fairly thick boundaries and have no homeotropic texture (Fig. 5(a)). Therefore optical observations suggest a highly ordered mesophase, which is compatible with a soft crystal phase of G or J type. Phase transition temperatures of these compounds are obtained from DSC thermograms and are given in Table 3. The enthalpies of clearing are higher than those of melting, except for $n = 18$. Again a highly ordered mesophase is suggested. The technique of powder XRD was employed to better understand the mesomorphic structure of these compounds. The diffractogram of $[Cu(C_{18}H_{37}\text{-im})_4][NO_3]_2$ at 100 °C in the mesophase, shows a strong reflection at 38.4 Å and weak reflections at 19.1, 12.7 and 9.4 Å of equal spacing, followed by weak reflections at 8.0 Å and several weak peaks including a halo at medium angle (Fig. 5(b)). This result suggests the presence of a mesophase, which adopts a lamellar structure with a layer distance of 38.4 Å and a long-range order in the layer plane. The small increment (2.9 Å) of the layer spacing from the solid (35.5 Å) to the mesophase (38.4 Å) indicates the presence of similar non-interdigitated monolayer

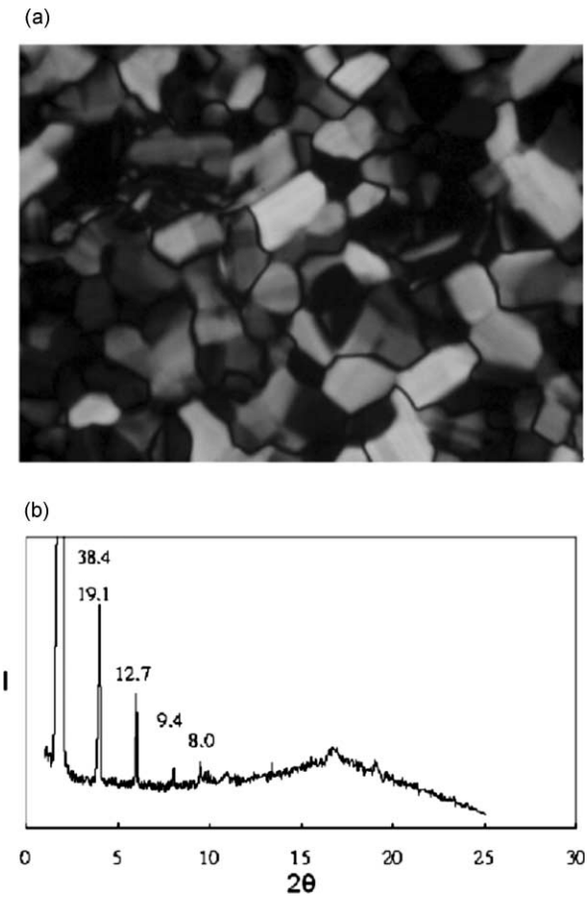

Fig. 5 (a) The mosaic texture of $[Cu(C_{18}H_{37}\text{-im})_4][NO_3]_2$ at 145 °C from POM. (b) Powder XRD of $[Cu(C_{18}H_{37}\text{-im})_4][NO_3]_2$ at 100 °C.

lamellae in the solid phase and the mesophase. Using the structural data from the ionic Cu(II) compound as a model, the 8.0 Å reflection is caused by the rhombic Cu arrangement in this phase. Results from POM, DSC and X-ray diffraction therefore, suggest a highly ordered mesophase of soft crystal of the type G or J. The ionic Cu(II) compounds with $n = 12$, 14 and 16 have similar diffractograms in the mesophase (*d* spacings in the solid and mesophase are given in Table 4). Therefore similar mesomorphic structures are proposed.

Conclusion

In this work, neutral and ionic *N*-alkylimidazole complexes were synthesized by the reaction of *N*-alkylimidazole with MCl_2 or $M(NO_3)_2$. Crystal structures of the non-mesomorphic $[Pd(C_{12}H_{25}\text{-im})_2Cl_2]$ and $[Cu(C_{12}H_{25}\text{-im})_2Cl_2]$ and mesomorphic $[Zn(C_{18}H_{37}\text{-im})_2Cl_2]$ and $[Cu(C_{12}H_{25}\text{-im})_4][NO_3]_2$ have been studied. All series of compounds in the solid state have a well defined monolayer lamellar structure except the series of $[Zn(C_nH_{2n+1}\text{-im})_2Cl_2]$ which adopts a bilayer stacking. All of these complexes are stable up to 200 °C. The ionic complexes have lower melting temperature than those of the neutral complexes. Between the two ionic Zn(II) and Cu(II) series, the former has lower phase transition temperatures than those of the latter. Possibly the tetrahedral Zn(II) compounds have weaker intermolecular core–core interactions than those of the square-planar Cu(II) compounds due to steric reasons. Crystal structural results of these complexes may provide a model for the molecular arrangement of organic–inorganic hybrid materials in the solid state and mesophase.

Experimental

Solvents were reagent grade from Mallinckrodt Chemical Co. and were used without further purification, except for THF,

which was dried by standard techniques. Imidazoles were purchased from R. D. H. Alkyl halides were obtained from TCI. C_nH_{2n+1}-im were prepared according to the literature.[11] The ^{1}H NMR spectra were recorded on a Bruker AC-F300 spectrometer in $CDCl_3$ with tetramethylsilane as an internal standard. Elemental microanalyses were performed by the Taiwan Instrumentation Center. Optical characterization was performed on an Olympus BH-2 polarizing microscope equipped with Mettler FP 82 hot stage and Mettler FP 90 central processor. Transition temperatures and heats of fusion were determined by differential scanning calorimetry using a Perkin-Elmer DSC-7 calorimeter, which was calibrated with indium and tin standards in conjunction with a Perkin-Elmer 7700 thermal analysis data station. The powder diffraction data were collected from the Wiggler-A beamline of the National Synchrotron Radiation Research Center (NSRRC).[13] Diffraction patterns were recorded in $\theta/2\theta$ geometry with step scans normally 0.02° in 2θ = 1–10° step^{-1} s^{-1} and 0.05° in 2θ = 10–25° step^{-1} s^{-1}and a gas flow heater was used to control the temperature. The powder samples were charged in Lindemann capillary tubes (80 mm long and 0.01 mm thick) from Charles Supper Co. with an inner diameter of 0.10 or 0.15 mm.

X-Ray crystallography

Single crystal X-ray data for $[Pd(C_{12}H_{25}\text{-im})_2Cl_2]$, $[Cu(C_{12}H_{25}\text{-im})_2Cl_2]$, $[Cu(C_{12}H_{25}\text{-im})_4][NO_3]_2$ were collected on a Bruker SMART diffractometer equipped with a CCD area detector with graphite-monochromated Mo-Kα radiation and $[Zn(C_{18}H_{37}\text{-im})_2Cl_2]$ was collected on a Bruker P4 diffractometer equipped with a graphite monochromator using Mo-Kα radiation. Details of crystal parameters, data collection and structure refinements are summarized in Table 1. All structures were solved and refined using SHELX97.[14] All non-hydrogen atoms were refined anisotropically. In all cases, hydrogen atoms were placed in calculated positions and allowed to ride on their parent atoms. The large $R1$ value (0.0749) for $[Zn(C_{18}H_{37}\text{-im})_2Cl_2]$ is due to the poor quality of the crystal and only low intensity reflections were obtained. The preliminary structure of $[Cu(C_{12}H_{25}\text{-im})_4][NO_3]_2$ is resolved, but the crystal quality is poor due to the disordering of two alkyl chains. Detailed information of this structure is supplied in the ESI. †

CCDC reference numbers 216100–216102.

See http://www.rsc.org/suppdata/dt/b3/b308648h/ for crystallographic data in CIF or other electronic format.

Preparation of metal complexes

Dichlorobis(1-dodecylimidazole)paladium(II), $[Pd(C_{12}H_{25}\text{-im})_2Cl_2]$. To a CH_2Cl_2 solution (30 mL) of 1-dodecylimidazole (1.0 g, 4.2 mmol) was added an acetone solution of $Pd(CH_3CN)_2Cl_2$ (0.55 g, 2.1 mmol), and this mixture was stirred for 5 min at room temperature. The solvent was then removed under vacuum. The product as an orange solid was obtained after recrystallization from dichloromethane–acetone. The yield was >90%. ^{1}H NMR (ppm, $CDCl_3$): δ 0.88 (t, ^3J = 7 Hz, CH_3, 3H), 1.18–1.33 (m, CH_2, 30H), 1.75 (m, CH_2, 2H), 3.89 (t, ^3J = 7 Hz, NCH_2, 2H), 6.78 (s, CH, 1H), 7.40 (s, CH, 1H), 7.99 (s, CH, 1H). Anal. Calc. for $PdC_{30}H_{56}N_4Cl_2$: C 55.42; H 8.68; N 8.62. Found: C 55.05; H 8.59; N 8.57%. Data for the compounds with n = 10 and 18 are given as ESI. †

Dichlorobis(1-dodecylimidazole)copper(II), $[Cu(C_{12}H_{25}\text{-im})_2Cl_2]$. To an ethanol solution (30 mL) of 1-dodecylimidazole (1.0 g, 4.2 mmol) was added an ethanol solution of $CuCl_2$ (0.28 g, 2.1 mmol). This mixture was stirred for 5 min at room temperature. The solvent was then removed under vacuum. The product was obtained as a blue solid after recrystallization from dichloromethane–acetone. The yield was >90%. Anal. Calc. for $CuC_{30}H_{56}N_4Cl_2$: C 59.34; H 9.30; N 9.23. Found: C 59.28; H 9.36; N 9.10%.

$[Cu(C_{18}H_{37}\text{-im})_2Cl_2]$. Anal. Calc. for $CuC_{42}H_{80}N_4Cl_2$: C 65.16; H 10.42; N 7.24. Found: C 64.94; H 10.39; N 7.30%.

Dichlorobis(1-dodecylimidazole)zinc(II), $[Zn(C_{12}H_{25}\text{-im})_2Cl_2]$. To an ethanol solution (30 mL) of 1-dodecylimidazole (1.0 g, 4.2 mmol) was added an ethanol solution of $ZnCl_2$ (0.29 g, 2.1 mmol). This mixture was stirred for 5 min at room temperature, after which the solvent was removed under vacuum. A white solid was obtained after recrystallization from dichloromethane–ether. The yield was >90%. ^{1}H NMR (ppm, $CDCl_3$): δ 0.87 (t, ^3J = 7 Hz, CH_3, 3H), 1.18–1.33 (m, CH_2, 30H), 1.79 (m, CH_2, 2H), 3.97 (t, ^3J = 7 Hz, NCH_2, 2H), 6.98 (s, CH, 1H), 7.15 (s, CH, 1H), 7.98 (s, CH, 1H). Anal. Calc. for $ZnC_{30}H_{56}N_4Cl_2$: C 59.16; H 9.27; N 9.20. Found: C 58.95; H 9.27; N 9.12%.

$[Cu(C_{12}H_{25}\text{-im})_4][NO_3]_2$. To an ethanol solution (30 mL) of 1-dodecylimidazole (1.0 g, 4.2 mmol) was added an ethanol solution of $Cu(NO_3)_2{\cdot}2.5H_2O$ (0.25 g, 1.1 mmol), and this mixture was stirred for 5 min at room temperature. The solvent was then removed under vacuum. A blue solid product was obtained after recrystallization from dichloromethane–acetone. The yield was >90%. Anal. Calc. for $CuC_{60}H_{112}N_{10}O_6$: 63.62; H 9.97; N 12.37. Found: C 63.63; H 10.10; N 12.27%. Data for the compounds with n = 10, 14 and 16 are given as ESI. †

$[Zn(C_{12}H_{25}\text{-im})_4][NO_3]_2{\cdot}H_2O$. To an ethanol solution (30 mL) of 1-dodecylimidazole (1.0 g, 4.2 mmol) was added an ethanol solution of $Zn[NO_3]_2{\cdot}6H_2O$ (0.32 g, 1.1 mmol). After this mixture was stirred for 5 min at room temperature, the solvent was removed under vacuum. The colorless liquid was washed several times with water and ether. The yield was >90 %. ^{1}H NMR (ppm, $CDCl_3$): δ 0.88 (t, ^3J = 7 Hz, CH_3, 3H), 1.18–1.33 (m, CH_2, 30H), 1.80 (m, CH_2, 2H), 4.03 (t, ^3J = 7 Hz, NCH_2, 2H), 6.99 (s, CH, 1H), 7.25 (s, CH, 1H), 8.26 (s, CH, 1H). Anal. Calc. for $ZnC_{60}H_{114}N_{10}O_7$: C 62.56; H 9.98; N 12.17. Found: C 62.12; H 9.83; N 12.23%. Data for the compounds with n = 8, 10, 14, 16 and 18 are given as ESI. †

Acknowledgements

We thank The National Synchrotron Radiation Research Center (NSRRC) for the powder X-ray diffraction measurements. We also thank Dr. K. M. Lee for the characterization of one crystal structure. A research grant (NSC92-2113-M-259-008) from National Science Council of Taiwan is greatly appreciated.

References

1 D. B. Mitzi, *Chem. Mater.*, 2001, **13**, 3283.
2 P. Rabu and M. Drillon, *Adv. Eng. Mater.*, 2003, **5**, 189.
3 K. E. Gonsalves, L. Merhari, H. Wu and Y. Hu, *Adv. Mater.*, 2001, **13**, 703.
4 P. Gomez-Romero, *Adv. Mater.*, 2001, **13**, 63.
5 I. O. Benítez, B. Bujoli, L. J. Camus, C. M. Lee, F. Odobel and D. R. Talham, *J. Am. Chem. Soc.*, 2002, **124**, 4363.
6 A. K. Kakkar, *Chem. Rev.*, 2002, **102**, 3579–3588.
7 I. Kuzmenko, H. Rapaport, K. Kjaer, J. Als-Nielsen, I. Weissbuch, M. Lahav and L. Leiserowitz, *Chem. Rev.*, 2001, **101**, 1659.
8 (*a*) D. Demus, J. Goodby, G. W. Gray, H. W. Spiess and V. Vill, *Handbook of Liquid Crystals*, Wiley-VCH, New York, 1998; (*b*) F. Neve, *Adv. Mater.*, 1996, **8**, 277; (*c*) J. L. Serrano, *Metallomesogen*, VCH, Weinheim, 1996; (*d*) R. W. Date, E. F. Iglesias, K. E. Rowe, J. M. Elliott and D. W. Bruce, *Dalton Trans.*, 2003, 1914.
9 (*a*) C. J. Bowlas, D. W. Bruce and K. R. Seddon, *Chem. Commun.*, 1996, 1625; (*b*) F. Neve, A. Crispini, S. Armentano and O. Francescangeli, *Chem. Mater.*, 1980, **10**, 1904; (*c*) F. Neve, O. Francescangeli and A. Crispini, *Inorg Chem. Acta*, 2002, **338**, 51; (*d*) F. Neve, A. Crispini and O. Francescangeli, *Inorg. Chem.*, 2000, **39**, 1187; (*e*) F. Neve, O. Francescangeli, A. Crispini and J. Charmant, *Chem. Mater.*, 2001, **13**, 2032.

10 (*a*) T. G. Traylor, D. Magde, J. Marsters, K. Jongeward, G.-Z. Wu and K. Walda, *J. Am. Chem. Soc.*, 1993, **115**, 4808; (*b*) W. N. Cannon, C. E. Powell and R. G. Jones, *J. Org. Chem.*, 1957, **22**, 1323.
11 C. K. Johnson, ORTEP-II: A FORTRAN Thermal Ellipsoid Plot Program for Crystal Structure Illustrations, Report ORNL-5138, Oak Ridge National Laboratory, Oak Ridge, TN, USA, 1976.
12 (*a*) D. J. Abdallah, R. E. Bachman, J. Perlstein and R. G. Weiss, *J. Phys. Chem. B*, 1999, **103**, 9269; (*b*) D. J. Abdallah and R. G. Weiss, *Chem. Mater.*, 2000, **12**, 406; (*c*) H. Chen, D. C. Kwait, Z. S. Gönen, B. T. Weslowski, D. J. Abdallah and R. G. Weiss, *Chem. Mater.*, 2002, **14**, 4063, and references therein.
13 K. L. Tsang, C.-H. Lee, Y. C. Jean, T.-E. Dann, J. R. Chen, K. L. D'Amico and T. Oversluizen, *Rev. Sci. Instrum.*, 1995, **66**, 1812.
14 (*a*) G. M. Sheldrick, SHELXL-97, Program for refinement of crystal structures, University of Göttingen, Germany, 1997; (*b*) G. M. Sheldrick, SHELXS-97, Program for solution of crystal structures, University of Göttingen, Germany, 1997.